Author Manuscript

Author Manuscript

Author Manuscript

Author Manuscript

HHS Public Access

Author manuscript

Cancer Res. Author manuscript; available in PMC 2016 March 15.

Published in final edited form as:

Cancer Res. 2015 March 15; 75(6): 1046–1055. doi:10.1158/0008-5472.CAN-14-1851.

Interferon Regulatory Factor-1 signaling regulates the switch between autophagy and apoptosis to determine breast cancer cell fate

Jessica L. Schwartz-Roberts[1], **Katherine L. Cook**[1], **Chun Chen**[3], **Ayesha N. Shajahan-Haq**[1], **Margaret Axelrod**[1], **Anni Wärri**[1], **Rebecca B. Riggins**[1], **Lu Jin**[1], **Bassem R. Haddad**[1], **Bhaskar V. Kallakury**[2], **William T. Baumann**[3], and **Robert Clarke**[1,*]

[1]Departments of Physiology & Biophysics, and Oncology, Lombardi Comprehensive Cancer Center, Georgetown University, 3970 Reservoir Road NW, Washington, DC 20057, USA

[2]Department of Pathology, Georgetown University Medical Center, 3900 Reservoir Road NW, Washington, DC 20057, USA

[3]Department of Biological Sciences and Electrical & Computer Engineering, Virginia Polytechnic Institute & State University, Blacksburg, VA 24061, USA

Abstract

Interferon regulatory factor-1 (IRF1) is a tumor suppressor that regulates cell fate in several cell types. Here we report an inverse correlation in expression of nuclear IRF1 and the autophagy regulator ATG7 in human breast cancer cells that directly impacts their cell fate. In mice harboring mutant Atg7, nuclear IRF1 was increased in mammary tumors, spleen, and kidney. Mechanistic investigations identified ATG7 and the cell death modulator Beclin-1 (BECN1) as negative regulators of IRF1. Silencing ATG7 or BECN1 caused estrogen receptor-α (ERα) to exit the nucleus at the time when IRF1 nuclear localization occurred. Conversely, silencing IRF1 promoted autophagy by increasing BECN1 and blunting IGF-1 receptor and mTOR survival signaling. Loss of IRF1 promoted resistance to anti-estrogens, whereas combined silencing of ATG7 and IRF1 restored sensitivity to these agents. Using a mathematical model to prompt signaling hypotheses, we developed evidence that ATG7 silencing could resensitize IRF1-attenuated cells to apoptosis through mechanisms that involve other estrogen-regulated genes. Overall, our work shows how inhibiting the autophagy proteins ATG7 and BECN1 can regulate IRF1 dependent and independent signaling pathways in ways that engender a new therapeutic strategy to attack breast cancer.

Keywords

autophagy; IRF1; antiestrogen; breast cancer; apoptosis

*To whom correspondence should be addressed: Robert Clarke, PhD, DSc, Research Building W405A, Department of Oncology, 3970 Reservoir Road NW, Washington, DC 20057, USA; Tel: +1 202 687 3755; Fax: +1 202 687 7505; clarker@georgetown.edu.

Conflicts of Interest: The authors disclose no potential conflicts of interest.

Competing interests: The authors declare they have no competing interests.

Author Manuscript Author Manuscript Author Manuscript Author Manuscript

Introduction

Breast cancer remains one of the most prevalent cancers among American women (1). With more than 70% of these breast cancers expressing the estrogen receptor-α (ER+), many tumors depend on estrogen to drive cell proliferation and promote cell survival. The routine use of antiestrogens (AEs), such as tamoxifen (TAM) and fulvestrant (Faslodex; ICI 182,780; ICI), and aromatase inhibitors (AIs) including letrozole and anastrozole, are now established as effective therapies for the treatment of breast cancer (2, 3). The widespread use of endocrine therapy is a major contributor leading to the decline in breast cancer mortality in women with ER+ disease (4). However, clinical efficacy of these therapies is often limited by aberrations in prosurvival and prodeath signaling leading to drug resistance. Precisely how signaling within breast cancer cells regulates the cell fate decision in response to endocrine therapies remains largely unknown.

IRF1 is a nuclear transcription factor that is activated by many immune effector molecules including type I and type II (IFN-γ) interferons, tumor necrosis factor-α (TNF-α), retinoic acid, interleukin-1 (IL-1), IL-6, and in response to viral infection (5). Upon activation, IRF1 alters the transcriptional activity of genes involved in immunomodulation, antiviral responses, and tumor suppression (5, 6). Previous studies have established a role for IRF1 in inhibiting breast cancer cell growth including by opposing the actions of IRF2 and inducing apoptosis (7, 8). Furthermore, gene expression microarrays comparing antiestrogen-responsive (MCF7/LCC1) and -resistant (MCF7/LCC9) human breast cancer cell lines report that IRF1 is downregulated in resistant cells, suggesting that loss of IRF1 may contribute to endocrine resistance through its reduced ability to induce cell death (9-11). Indeed, IRF1 mRNA levels correlate with a pathologic complete response and reduced risk of recurrence and death in some breast cancers (12, 13). Recent evidence suggests that autophagy proteins have a major effect on the regulation of inflammatory transcriptional responses. Embryonic mice lacking the autophagy related 5 (*Atg5*) gene have increased inflammation in tissue with impaired clearance of apoptotic cells, raising the possibility that autophagy has a role in inflammation and autoimmunity (14).

A critical decision point in the determination of cell fate in response to endocrine therapies appears to be affected by the balance between autophagy (prosurvival) and apoptosis (prodeath) (15). The activities of IRF1 in multiple cell types suggests that it may be a key component in regulating cell fate decisions and perhaps a critical regulator of the switch between apoptosis and autophagy. Thus, we investigated the biological function of IRF1 in autophagy in the context of endocrine responsiveness in breast cancer. We established an important (inverse) link between ATG7 and IRF1 expression/function, which we confirmed using immunohistochemical studies in human breast carcinomas and tissue from *Atg7* +/- mice. We also showed that inhibition of the autophagy proteins ATG7 and BECN1 promoted IRF1 signaling and induced apoptotic cell death. Conversely, inhibition of IRF1 prolonged cell survival and promoted autophagy. Thus, our data suggest that IRF1 inhibits breast cancer cell growth through its ability to regulate both autophagy and apoptosis. To better understand the molecular interactions, we constructed an influence diagram of the novel signaling and then used this as a guide to build mathematical models using our experimental data. Model simulations suggested additional experimentation to distinguish

Author Manuscript Author Manuscript Author Manuscript Author Manuscript

whether ATG7 knockout promotes endocrine responsiveness through either IRF1-dependent or -independent signaling. Collectively, these data indicate a major role for IRF1 in regulating cell fate decisions in breast cancer and also establish an IRF1-independent path as a further signaling component in ATG7-mediated cell death.

Materials and Methods

Cell culture, reagents, and small interfering RNA (siRNA) treatments

MCF7, T47D, BT-474, and MDA-MB-231 cells were maintained in improved minimal essential media (IMEM) with phenol red and supplemented with 5% fetal bovine serum (Life Technologies). MCF7/LCC1 (LCC1) and MCF7/LCC9 (LCC9) cells were grown in phenol red-free IMEM supplemented with 5% charcoal-stripped calf serum. All cells were maintained in a humidified atmosphere at 37°C and 95% air/5% CO_2. ATG7 (SignalSilence; Cell Signaling Technology), BECN1 and STAT1 (three unique siRNAs for each target; OriGene), IRF1 (Silencer Select; consisting of 3 different siRNA for same target; Life Technologies), or control (Ctrl) siRNA were transfected in cells using Lipofectamine RNAiMAX (Life Technologies) according to the manufacturer's instructions. ERα and ATG7 cDNA were from Origene; ICI 182,780 (ICI; Faslodex; Fulvestrant) was from Tocris Bioscience; HCQ, 3-MA, and NAC were from Sigma-Aldrich and the JAK inhibitor 1 ($C_{19}H_{16}FN_3O$) was obtained from EMD Millipore.

Cell Proliferation

Cells were transfected with IRF1, ATG7, BECN1, or Ctrl siRNA and seeded at a density of 0.2×10^6 per well in 24-well plates. One day after plating, cells were treated with the indicated concentration of ICI or vehicle control. Cells were incubated with ICI for 6 days and then cell density was measured as previously described (10, 16).

Western blot analysis

Lysates were harvested from transfected cell monolayers and protein analysis was measured as previously described (17). Membranes were probed for proteins of interest at 4°C overnight. To confirm equal loading of the gels, membranes were reprobed for β-actin (1:1000; Santa Cruz Biotechnology).

MMP, autophagosome formation, and ROS assays

Cells were reverse transfected with ATG7, BECN1, IRF1, or Ctrl siRNA and plated in 6-well tissue culture plates. The following day, cells were treated with 100 nM ICI or vehicle control. Cells were harvested 48 hours later and stained as described in the Mitochondrial Permeability Detection Kit for flow cytometry (Enzo). Accumulation of autophagic vesicles was measured using a modified monodansylcadaverine according to the manufacturer's instructions (Enzo Cyto-ID Autophagy detection kit). Total reactive oxygen species (ROS) were stained according to Enzo's Total ROS Detection Kit instructions. Stained cells were detected and appropriate signals measured by fluorescence-activated cell sorting (LCCC FACS Shared Resource).

Author Manuscript Author Manuscript Author Manuscript Author Manuscript

Autophagosome maturation and localization studies

Cells (1×10^5) were reverse transfected with IRF1, ATG7, BECN1, or Ctrl siRNA and seeded onto 18 × 18 mm glass coverslips. The following day, IRF1 siRNA cells were transfected with LC3 tagged with a green fluorescent protein (GFP). 24 hours later, cells were treated with 500 nM ICI or vehicle, and then fixed and stained for IRF1 as previously described (11). IRF1 and ERα were also measured in LCC1 cells following knockdown of ATG7, BECN1, or IRF1 to determine subcellular localization.

Mathematical modeling and data fitting

Matlab (version 7.9.0) was used to build the mathematical model and perform simulations. An ordinary differential equation (ODE) formalism (18-20) was used to model the outcomes observed in experiments. Experimental data on cell proliferation under different conditions were used to fit the model by a least-squares approach. Further details of the model are described in Fig. S1.

In vivo experiments

Tumors from female *Atg7* +/- and wild-type (WT) mice (21) (Harlan, USA) were treated with medroxyprogesterone acetate (MPA, DepoProvera, Pfizer) and 7,12-dimethylbenz(a)anthracene (DMBA; Sigma) to induce mammary tumors, as described earlier (22). Mice were euthanized once tumors reached 10% of the mouse body size, or when a single tumor volume reached 1000 mm^3; mammary tumors and organs were removed at necroscopy, fixed in neutral buffered formalin, and processed using routine histological methods.

Human tissue microarrays

Human tissue microarrays (TMAs) were obtained from the Familial Cancer Registry (FCR) at Georgetown Lombardi Comprehensive Cancer Center. TMAs contained 107 cores from breast tumors of FCR participants (2 cores/subject) with a known BRCA1/2 mutation status (known BRCA1/2 mutation carriers and non-carriers). The histologic diagnosis was confirmed by a pathologist at the time of the immunohistochemistry scoring. Patient/tumor characteristics are shown in Table S1.

Immunohistochemistry

Five-micron sections from paraffin embedded human TMAs and mouse mammary tissue were stained with mouse anti-IRF1 (1:100; BD Biosciences) or rabbit anti-APG7 (1:130; Santa Cruz Biotechnology) antibodies as previously described (17). Assessments of immunohistochemical staining was performed by a pathologist blinded both to the clinical and molecular data. Cytoplasmic and nuclear staining of ATG7 and IRF1 were described in terms of intensity (0: negative, 1+: weak, 2+: intermediate, 3+: strong) and distribution (0: negative, +1: <10%, 2+: 11-50%; 3+: >50%). A simplified total immunohistochemistry score (the sum of the intensity and distribution scores) was calculated for each core. For *in vivo* staining, a computer-assisted counting technique with a grid filter to select cells was used to quantify the immunohistochemical staining of IRF1 (23). Cells stained positive were

Author Manuscript Author Manuscript Author Manuscript Author Manuscript

expressed as a percentage of the total cell number examined (100 cells sampled from each tissue site within each breast tumor section).

Statistical analysis

Prism 5.0 was used for statistical analysis. Differences between two groups were analyzed by Student t tests, and multiple group comparisons were assessed by one-way ANOVA followed by Bonferroni *post hoc* tests. The Pearson correlation coefficient was calculated to measure the correlation between ATG7 and IRF1 in human tumor tissue. Differences were considered statistically significant at $P < 0.05$.

Results

Nuclear IRF1 and ATG7 are inversely correlated in vivo and in human breast cancer tissue

We used immunohistochemistry to study IRF1 expression in mammary tumors from wild-type (WT) mice and mice with a mutated *Atg7* allele (+/-); *Atg7* null mice (-/-) are not viable (21). 98% of breast adenocarcinoma tumors generated by this model were ER+. Mammary tumors, spleen, and kidney from *Atg7* +/- mice exhibited increased nuclear IRF1 staining (arrows in Fig. 1A) compared with their WT controls (Fig. 1A; $P < 0.001$). We then examined whether nuclear IRF1 protein expression was associated with ATG7 protein expression in human disease by staining TMAs containing n=107 cores from breast tumors. Since only nuclear IRF1 is likely to be transcriptionally active, we scored separately nuclear and cytoplasmic IRF1 staining (24). We found the primary form of IRF1 to be cytoplasmic (expressed in 80% of cases), while nuclear IRF1 was only detected in 13% (14/107) of tumors. Furthermore, we found that >96% of samples (90/94) with positive ATG7 expression had low or undetectable nuclear IRF1 expression (Fig. 1B and C). Conversely, >70% of samples (10/14) with nuclear IRF1 expression had low ATG7 expression. An inverse correlation was found between ATG7 and nuclear IRF1 expression in these human breast tumors (Fig. 1C; $r = -0.28$, $P < 0.01$). We then examined the expression of IRF1 and ATG7 in ER+ and ER- human breast tumors using immunohistochemistry. ER status was identified in 52 out of the 107 human breast cancer cores. ER+ tumors exhibited significantly greater ATG7 ($P < 0.001$) and decreased nuclear IRF1 ($P < 0.01$) expression when compared with ER- tumors (Fig. 1D and Table S2), suggesting that the reduced nuclear IRF1 expression in ER+ breast tumors may be functionally related to increased ATG7 expression.

ATG7 and BECN1 knockdown stimulates IRF1 expression

Since a putative link was established between IRF1 and ATG7, we used various inhibitors and siRNA targeting of ATG7 and other key autophagy proteins in breast cancer cell lines and measured IRF1 protein expression. Antiestrogen sensitive LCC1 cells were treated with vehicle (control), 100 nM ICI, 5 mM 3-methyladenine (3-MA), 10 μM hydroxychloroquine (HCQ), or reverse transfected with ATG5, ATG7, or beclin-1 (BECN1) siRNA (Fig. 2A) for 48 hours before total protein was harvested. ATG5 and ATG7 are both involved in autophagosome membrane formation and elongation (14, 15). Levels of IRF1 protein were measured in breast cancer cell lines with deficient autophagy and were found to be significantly elevated in LCC1 cells with reduced ATG7 and BECN1 (Fig. 2A; $P < 0.001$).

Author Manuscript Author Manuscript Author Manuscript Author Manuscript

When further studied in other ER+ breast cancer cell lines including MCF7 (antiestrogen-sensitive), LCC9 (antiestrogen-resistant), T47D (antiestrogen-sensitive, p53 mutant), and BT-474 (antiestrogen-sensitive, HER2 amplified), we observed that ATG7 and BECN1 knockout cells (except ATG7 knockout in BT-474 cells) had elevated expression of IRF1 compared with control cells (Fig. 2B and C). We further determined that ATG7 and BECN1 siRNA induced apoptosis in LCC1 and LCC9 cells as measured by an increase in mitochondrial membrane permeability (Fig. 2D). However, the ER- cell line MDA-MB-231 did not exhibit enhanced IRF1 expression following transfection with either ATG7 or BECN1 siRNA (Fig. 2E). We then overexpressed ATG7 in LCC1 cells and found that ectopic expression of ATG7 significantly reduced IRF1 expression (Fig. 2F; $P < 0.05$). These results suggest that ER+ breast cancer cells may use autophagy machinery (ATG7 and BECN1) to regulate IRF1 expression and block apoptosis.

IRF1 localizes to the nucleus following ATG7 and BECN1 knockdown

To examine further the relationships among IRF1, ATG7/BECN1, and ER status, we used confocal microscopy to establish the subcellular localization of IRF1 and ERα following ATG7 and BECN1 knockdown. ER+ LCC1 cells were transfected with IRF1, ATG7, BECN1, or control (Ctrl) siRNA for 48 hours and stained for IRF1 (green) and ERα (red); DAPI (blue) staining indicates nuclear localization (Fig. 3A). In LCC1 control cells, IRF1 and ERα were predominantly localized in the nucleus and a significant amount of each co-localized (Fig. 3A). Transfection with ATG7 or BECN1 siRNA enhanced the nuclear expression of IRF1; however, ERα was no longer detected in nuclei that had IRF1 induced by siATG7 and siBECN1 (Fig. 3A). These results were further confirmed by detecting increased IRF1 in the nuclear fraction of LCC1 and LCC9 cells transfected with ATG7 or BECN1 siRNA (Fig. S2).

Protein expression of antiapoptotic BCL2 is induced by 17β-estradiol, whereas BCL2 promoter activity is reduced by IRF1 (11). We measured BCL2 protein expression in LCC1 and LCC9 cells transfected with ATG7, BECN1, or Ctrl siRNA. Knockdown of BECN1 significantly inhibited BCL2 expression in LCC1 and LCC9 cells, whereas knockdown of ATG7 only reduced BCL2 in LCC1 cells (Fig. 3B and C). The association between ERα and IRF1 was further investigated by measuring basal ERα and IRF1 protein levels in MDA-MB-231 (231-wt), and MDA-MB-231 cells transfected with a full length ERα cDNA (231-ER). 231-ER cells had 1/3 less IRF1 expression compared with their 231-wt counterparts ($P < 0.05$; Fig. 3D). These data strongly support a functional link between ER-mediated IRF1 regulation and BCL2 repression in autophagy-deficient breast cancer cells.

We also investigated whether inhibition of the Janus kinase/signal transducers and activators of transcription (JAK/STAT) pathway would block IRF1 expression in LCC1 cells deficient in ATG7 and BECN1. Despite inhibition of STAT1 and STAT2, IRF1 remained elevated in ATG7 (Fig. 3E) and BECN1 knockdown cells (Fig. 3F). IRF1 gene expression is also regulated by reactive oxygen species (ROS) formation (25). LCC1 cells transfected with ATG7 siRNA had increased levels of ROS compared with control-transfected cells (Fig. S3). Treatment with 5 mM N-acetylcysteine (NAC), an antioxidant that suppresses ROS, had no effect on IRF1 suppression in ATG7 deficient cells (Fig. S3). Collectively, these data

Author Manuscript Author Manuscript Author Manuscript Author Manuscript

demonstrate that ATG7 and BECN1 regulate IRF1 through STAT1/2- and ROS-independent mechanisms.

Knockdown of IRF1 stimulates autophagy

LCC1 and LCC9 cells were transfected with IRF1 or Ctrl siRNA and treated with vehicle or 100 nM ICI for 48 hours. Consistent with previous reports (11), we found increased levels of BCL2 when IRF1 was repressed (Fig. 4A). Western blotting also demonstrated that the total expression of LC3B-II (the lipidated form of LC3 found in autophagosome membranes) was increased in LCC1 and LCC9 cells expressing little to no detectable IRF1 (Fig. 4A). Furthermore, expression of p62 (an autophagic cargo marker degraded in the final stages of autophagy) was reduced in LCC1 cells transfected with IRF1 siRNA (Fig. 4A).

We used confocal microscopy and flow cytometry to confirm that breast cancer cells with reduced IRF1 have enhanced autophagic vacuole formation. While ICI slightly enhanced autophagosome formation ($P < 0.05$), cells transfected with IRF1 siRNA had significantly higher numbers of autophagic vacuoles ($P < 0.001$) compared with Ctrl siRNA treated cells (Fig. 4B). By immunofluorescence, we measured LC3 punctae formation in LCC1 cells transfected with IRF1 or Ctrl siRNA (Fig. 4C). IRF1 knockdown cells showed elevated LC3 punctae compared with control cells. In contrast, overexpression of IRF1 in LCC9 cells resulted in an accumulation of p62 (Fig. 4D). Taken together, these results suggest that IRF1 inhibits autophagy through modulation of autophagy.

To identify autophagy effectors downstream of IRF1 action, we measured the expression of selected autophagy and growth factor proteins in LCC1 and LCC9 cells transfected with IRF1 or Ctrl siRNA. BECN1 contains an interferon-stimulated response element (ISRE) in its promoter and is negatively regulated by IRF1 in LCC1 cells (Fig. S3A-C). Stimulation of mTOR inhibits the initiation of autophagy and acts downstream of insulin-like growth factor 1 receptor (IGF1R) (15). Knockdown of IRF1 with siRNA inhibited IGF1R and mTOR protein expression (Fig. S4A-C). These findings suggest that IRF1 may inhibit autophagy through alteration of the IGF1R/mTOR and BECN1 pathway.

Mathematical modeling of IRF1-related signaling data

We next determined how silencing ATG7 and/or IRF1 affects ICI responsiveness in antiestrogen sensitive breast cancer cells. Loss of antiestrogen sensitivity with dominant-negative IRF1 (dnIRF1) was confirmed by crystal violet assay (Fig. S5). To establish that IRF1 siRNA had the same effect on ICI responsiveness, we measured the effect of IRF1 knockdown on ICI-mediated inhibition of cell density (Fig. 5A). Western blot analysis confirmed that IRF1 and ATG7 successfully inhibited expression of the appropriate target (Fig. 5A-B). LCC1 cells transfected with IRF1 siRNA were markedly less sensitive to growth inhibition by 10-1000 nM ICI treatment compared with Ctrl siRNA transfected cells (Fig. 5A; $P < 0.05$). Cells were then transfected with ATG7 siRNA alone and in combination with IRF1 siRNA to determine whether ATG7 knockdown could resensitize IRF1-deficient cells to ICI. While IRF1 siRNA blocked ICI responsiveness, LCC1 cells were growth inhibited by ATG7 siRNA alone, which was further decreased by 100 nM ICI

Author Manuscript Author Manuscript Author Manuscript Author Manuscript

treatment (Fig. 5B). LCC1 cells with silenced IRF1 and ATG7 had restored sensitivity to 100 nM ICI compared with cells transfected with IRF1 siRNA (Fig. 5B; $P < 0.001$).

To both capture and quantitatively understand the experimental data detailed above, we created a phenomenological mathematical model of LCC1 cells based on the key molecular components (ERα, IRF1, ATG7) and their interactions (Fig. 5C). The model was used to predict the effect of further knocking down ATG7 and IRF1, respectively. The model predictions in Fig. 5D and E shows that an increase in siATG7 concentration would not significantly affect the results, whereas increasing the siIRF1 concentration should increase the proliferation in response to ICI for both the siIRF1 and siIRF1+siATG7 cases (Fig. 5E). We then experimentally validated these model predictions by repeating the study with an increased concentration of siIRF1. Fig. S6 shows that the higher concentration of siIRF1 further reduced IRF1 protein expression without effecting cell density. Fig. 5F shows that siIRF1+siATG7 still results in ICI sensitivity, suggesting that ATG7 knockdown activates cell death through both IRF1-dependent and -independent mechanisms.

High IRF1 expression is associated with prolonged survival

Since IRF1 promotes AE sensitivity, we investigated the relationship between high and low IRF1 expression and breast cancer-specific survival among several patient datasets. Using the dataset by Wang *et al.* (26), we found that high IRF1 expression is associated with prolonged survival in the total population of breast cancer patients analyzed (Fig. 6A) and in the ER+ subgroup only (Fig. 6B). We also analyzed a combination of clinical datasets and found that high IRF1 expression is associated with prolonged survival in over 1600 patients (Fig. 6C) and in a smaller subset of ER- patients (Fig. 6D). These findings suggest that activation of IRF1 may be important for improved patient survival.

Discussion

The results presented here reveal that IRF1 is a critical signaling protein that contributes to the switch between apoptosis and autophagy to determine breast cancer cell fate. Upregulation of autophagy has been shown to protect breast cancer cells from antiestrogens (15). Previous studies also report that IRF1 mediates the antiproliferative and proapoptotic effects in cancer cells (9, 10, 27-29). Thus, we investigated the relationship between nuclear IRF1 and the key autophagy protein, ATG7, *in vivo* and in human breast cancer. *Atg7*-deficient mice exhibited increased nuclear IRF1 staining in DMBA-induced mammary tumors, kidney, and spleen, suggesting a broad role for IRF1 in autophagy signaling. Immunohistochemical staining of IRF1 in human breast tumors was broadly consistent with a study by Zhu *et al.*, further supporting a tumor suppressive role for IRF1 (24). ATG7 expression was detected in nearly all tumors. Since autophagy has a prosurvival role in breast cancer, ATG7 expression could enhance the aggressiveness of breast cancer cells and their ability to block proapoptotic stimuli. Furthermore, ATG7 could negatively regulate the activation state of IRF1 to alter breast cancer aggressiveness and response to therapy. Interestingly, we found that ER- tumor cells expressed detectable (1+ and higher) nuclear IRF1 staining compared with ER+ breast tumor cells. These findings suggested that some

Author Manuscript Author Manuscript Author Manuscript Author Manuscript

breast tumors may differentially regulate the activation state/subcellular localization of IRF1 through modulation of ATG7 and ERα.

We are the first to show that silencing the autophagy proteins, ATG7 and BECN1, induced IRF1 and restored drug sensitivity to ICI. Previous studies have reported that nude mice with *atg5*-deficient thymi showed massive inflammatory infiltrates, suggesting autophagy negatively regulated T-cell activation (30, 31). While we did not observe IRF1 induction with the autophagy inhibitors 3-MA, HCQ, or ATG5 siRNA, ATG7 and BECN1 may target different immunologic signaling molecules, specifically IRF1. We also found little to no IRF1 induction in BT-474 or MDA-MB-231 cells when either ATG7 or BECN1 was silenced (Fig. 2). BT-474 cells have amplified HER2, and in 3T3 cells transduced with Her2/neu, IRF1 became constitutively active (5). Thus, BT-474 cells may have constitutively active IRF1, and knockdown of ATG7 with siRNA had no additional effect on IRF1 activation. Wild type MDA-MB-231 cells do not express ERα; thus, IRF1 induction by ATG7 and BECN1 may be partly due to ERα regulation.

We found that knockdown of ATG7 sensitized antiestrogen resistant breast cancer cells to ICI through mechanisms involving ERα and IRF1. Silencing of ATG7 and BECN1 caused ERα to exit and IRF1 to enter the nucleus (Fig. 3A). It is possible that ERα was inactivated or degraded while IRF1 was activated in response to ATG7 and BECN1 knockdown. However, the role of altered receptor coactivator or corepressor expression in this situation is still unclear. For example, the transcription factor p300 can regulate IRF1 promoter activity and acts synergistically with ERα (32). Examining the role of other coactivators/corepressors is ongoing. IRF1 also inhibited BCL2 protein expression when either ATG7 or BECN1 was silenced (Fig. 3B and C). This observation is clinically important because TAM-resistant breast tumors have sustained BCL2 expression (33, 34). We previously showed that inhibiting BCL2 with the BH3 mimetic, GX15-070 (obatoclax), in combination with an antiestrogen successfully inhibited breast cancer cell growth through modulation of apoptosis and autophagy (16).

While IRF1 promotes apoptosis (10), we established that loss of IRF1 enhanced autophagy in human breast cancer cells. IRF1 inhibited autophagic vacuole formation and reduced BECN1 protein expression (Figs. 3B-D). BECN1 contains an interferon regulated response element sequence and is regulated by BCL2 (35), suggesting a possible interaction between IRF1 and BECN1. These data suggested that IRF1 might play a role in enhancing cell death by preventing autophagic cargo degradation. To further delineate how IRF1 inhibited the initiation of autophagy, we examined the expression of selected proteins to find downstream targets modified by loss of IRF1. IGF1R is implicated in autophagy signaling and can also promote endocrine resistance (36). IRF1 was necessary for IGF1R protein stability (Fig. S4B-D), suggesting that IRF1 can disrupt IGF1R/mTOR-mediated autophagy (Fig. S4B-D). IRF1 was previously shown to inhibit the autophagic response in lipopolysaccharide-stimulated macrophages by modulating the activation of mTOR (37).

Using our experimental data, we constructed two mathematical models fitting the observation that silencing ATG7 or BECN1 can block the effect of IRF1 siRNA on ICI responsiveness. To select the most correct model, an experiment for which the models

Author Manuscript Author Manuscript Author Manuscript Author Manuscript

predicted different results was identified and run, illustrating the usefulness of mathematical modeling to help evaluate complex biological behaviors and prioritize experiments. The new experimental results supported the view that ATG7 knockdown could also resensitize IRF1-deficient cells to ICI through an IRF1-independent mechanism. This could be due to a switch from autophagy to apoptosis and be mediated by other proteins that are shared between pathways, such as BCL2 (38). It is also possible that silencing ATG7 activated other cell death pathways such as necroptosis or an ER-mediated stress pathway (39, 40). Our co-localization studies also supported the modeling by showing that ERα left the nucleus and stimulated nuclear IRF1 expression following ATG7 knockdown.

Previous reports suggest that high mRNA levels of IRF1 are a marker for good prognosis for breast cancer patients given neoadjuvant treatment (12, 41). We now show that high IRF1 expression contributes to prolonged survival in over 1600 cases, highlighting the potential for IRF1 activation in the clinical setting. Furthermore, restoring IRF1 expression or controlling its modulation may be useful for the treatment of both ER+ and ER- breast tumors. Since IFNγ has produced mixed results as an antitumor agent in the clinic (5), using newer compounds that activate IRF1, such as baicalein might restore IRF1 activity and lead to better outcomes for some patients (42). We now show that inhibiting key autophagy proteins, ATG7 and BECN1 also induces IRF1, which could provide a possible therapeutic option. This novel ATG7/IRF1 axis provides new insight into the mechanisms underlying antiestrogen resistance, and implicates restoration of IRF1 as a potential therapeutic strategy for the treatment of breast cancer.

Supplementary Material

Refer to Web version on PubMed Central for supplementary material.

Acknowledgments

Assistance was provided by the Nontherapeutic Subject Registry (Familial Cancer Registry), Microscopy and Imaging, Flow Cytometry, Histopathology & Tissue, and Tissue Culture Shared Resources at Georgetown University Medical Center. These shared resources are partially supported by the NIH/NCI Cancer Center Support Grant (CCSG) P30-CA051008. We thank Dr. J.H. Yim (City of Hope) for critically reviewing this manuscript. We also thank Drs. M. Liu, T. Sherman, and P. Furth for their guidance and support.

Financial Support: This work was supported by Public Health Service Awards U54-CA149147, R01-CA131465, and Susan G. Komen Grant KG090245 to R. Clarke. J.L. Schwartz-Roberts is the recipient of NIH training grant F31CA165514-01A1 that also supported this research study.

Funding: This work was supported by Public Health Service Awards U54-CA149147, R01-CA131465, and Susan G. Komen Grant KG090245 to R.C. J.L.S.-R. is the recipient of NIH training grant F31CA165514-01A1 that also supported this research study.

References and Notes

1. Siegel R, Naishadham D, Jemal A. Cancer statistics, 2012. CA: a cancer journal for clinicians. 2012; 62:10–29. [PubMed: 22237781]
2. Howell A. Fulvestrant (‘Faslodex’): current and future role in breast cancer management. Critical reviews in oncology/hematology. 2006; 57:265–73. [PubMed: 16473018]
3. Riggins RB, Bouton AH, Liu MC, Clarke R. Antiestrogens, aromatase inhibitors, and apoptosis in breast cancer. Vitamins and hormones. 2005; 71:201–37. [PubMed: 16112269]

Author Manuscript Author Manuscript Author Manuscript Author Manuscript

4. Hurvitz SA, Pietras RJ. Rational management of endocrine resistance in breast cancer: a comprehensive review of estrogen receptor biology, treatment options, and future directions. Cancer. 2008; 113:2385–97. [PubMed: 18819158]
5. Schwartz JL, Shajahan AN, Clarke R. The Role of Interferon Regulatory Factor-1 (IRF1) in Overcoming Antiestrogen Resistance in the Treatment of Breast Cancer. International journal of breast cancer. 2011; 2011:912102. [PubMed: 22295238]
6. Kroger A, Dallugge A, Kirchhoff S, Hauser H. IRF-1 reverts the transformed phenotype of oncogenically transformed cells in vitro and in vivo. Oncogene. 2003; 22:1045–56. [PubMed: 12592391]
7. Yim JH, Ro SH, Lowney JK, Wu SJ, Connett J, Doherty GM. The role of interferon regulatory factor-1 and interferon regulatory factor-2 in IFN-gamma growth inhibition of human breast carcinoma cell lines. Journal of interferon & cytokine research : the official journal of the International Society for Interferon and Cytokine Research. 2003; 23:501–11.
8. Kim PK, Armstrong M, Liu Y, Yan P, Bucher B, Zuckerbraun BS, et al. IRF-1 expression induces apoptosis and inhibits tumor growth in mouse mammary cancer cells in vitro and in vivo. Oncogene. 2004; 23:1125–35. [PubMed: 14762441]
9. Bowie ML, Dietze EC, Delrow J, Bean GR, Troch MM, Marjoram RJ, et al. Interferon-regulatory factor-1 is critical for tamoxifen-mediated apoptosis in human mammary epithelial cells. Oncogene. 2004; 23:8743–55. [PubMed: 15467738]
10. Bouker KB, Skaar TC, Riggins RB, Harburger DS, Fernandez DR, Zwart A, et al. Interferon regulatory factor-1 (IRF-1) exhibits tumor suppressor activities in breast cancer associated with caspase activation and induction of apoptosis. Carcinogenesis. 2005; 26:1527–35. [PubMed: 15878912]
11. Ning Y, Riggins RB, Mulla JE, Chung H, Zwart A, Clarke R. IFNgamma restores breast cancer sensitivity to fulvestrant by regulating STAT1, IFN regulatory factor 1, NF-kappaB, BCL2 family members, and signaling to caspase-dependent apoptosis. Molecular cancer therapeutics. 2010; 9:1274–85. [PubMed: 20457620]
12. Kolacinska A, Fendler W, Szemraj J, Szymanska B, Borowska-Garganisz E, Nowik M, et al. Gene expression and pathologic response to neoadjuvant chemotherapy in breast cancer. Molecular biology reports. 2012; 39:7435–41. [PubMed: 22318550]
13. Cavalli LR, Riggins RB, Wang A, Clarke R, Haddad BR. Frequent loss of heterozygosity at the interferon regulatory factor-1 gene locus in breast cancer. Breast cancer research and treatment. 2010; 121:227–31. [PubMed: 19697121]
14. Qu X, Zou Z, Sun Q, Luby-Phelps K, Cheng P, Hogan RN, et al. Autophagy gene-dependent clearance of apoptotic cells during embryonic development. Cell. 2007; 128:931–46. [PubMed: 17350577]
15. Cook KL, Shajahan AN, Clarke R. Autophagy and endocrine resistance in breast cancer. Expert review of anticancer therapy. 2011; 11:1283–94. [PubMed: 21916582]
16. Schwartz-Roberts JL, Shajahan AN, Cook KL, Warri A, Abu-Asab M, Clarke R. GX15-070 (Obatoclax) Induces Apoptosis and Inhibits Cathepsin D- and L-Mediated Autophagosomal Lysis in Antiestrogen-Resistant Breast Cancer Cells. Molecular cancer therapeutics. 2013; 12:448–59. [PubMed: 23395885]
17. Cook KL, Shajahan AN, Warri A, Jin L, Hilakivi-Clarke LA, Clarke R. Glucose-regulated protein 78 controls cross-talk between apoptosis and autophagy to determine antiestrogen responsiveness. Cancer research. 2012; 72:3337–49. [PubMed: 22752300]
18. Tyson JJ, Novak B. Functional motifs in biochemical reaction networks. Annual review of physical chemistry. 2010; 61:219–40.
19. Mjolsness E, Sharp DH, Reinitz J. A connectionist model of development. Journal of theoretical biology. 1991; 152:429–53. [PubMed: 1758194]
20. Wilson HR, Cowan JD. Excitatory and inhibitory interactions in localized populations of model neurons. Biophysical journal. 1972; 12:1–24. [PubMed: 4332108]
21. Komatsu M, Waguri S, Ueno T, Iwata J, Murata S, Tanida I, et al. Impairment of starvation-induced and constitutive autophagy in Atg7-deficient mice. The Journal of cell biology. 2005; 169:425–34. [PubMed: 15866887]

Author Manuscript Author Manuscript Author Manuscript Author Manuscript

22. Yin Y, Bai R, Russell RG, Beildeck ME, Xie Z, Kopelovich L, et al. Characterization of medroxyprogesterone and DMBA-induced multilineage mammary tumors by gene expression profiling. Molecular carcinogenesis. 2005; 44:42–50. [PubMed: 15937957]
23. Stute P, Wood CE, Kaplan JR, Cline JM. Cyclic changes in the mammary gland of cynomolgus macaques. Fertility and sterility. 2004; 82(Suppl 3):1160–70. [PubMed: 15474090]
24. Zhu Y, Singh B, Hewitt S, Liu A, Gomez B, Wang A, et al. Expression patterns among interferon regulatory factor-1, human X-box binding protein-1, nuclear factor kappa B, nucleophosmin, estrogen receptor-alpha and progesterone receptor proteins in breast cancer tissue microarrays. International journal of oncology. 2006; 28:67–76. [PubMed: 16327981]
25. Liu T, Castro S, Brasier AR, Jamaluddin M, Garofalo RP, Casola A. Reactive oxygen species mediate virus-induced STAT activation: role of tyrosine phosphatases. The Journal of biological chemistry. 2004; 279:2461–9. [PubMed: 14578356]
26. Wang Y, Klijn JG, Zhang Y, Sieuwerts AM, Look MP, Yang F, et al. Gene-expression profiles to predict distant metastasis of lymph-node-negative primary breast cancer. Lancet. 2005; 365:671–9. [PubMed: 15721472]
27. Bouker KB, Skaar TC, Fernandez DR, O'Brien KA, Riggins RB, Cao D, et al. interferon regulatory factor-1 mediates the proapoptotic but not cell cycle arrest effects of the steroidal antiestrogen ICI 182,780 (faslodex, fulvestrant). Cancer research. 2004; 64:4030–9. [PubMed: 15173018]
28. Pizzoferrato E, Liu Y, Gambotto A, Armstrong MJ, Stang MT, Gooding WE, et al. Ectopic expression of interferon regulatory factor-1 promotes human breast cancer cell death and results in reduced expression of survivin. Cancer research. 2004; 64:8381–8. [PubMed: 15548708]
29. Stang MT, Armstrong MJ, Watson GA, Sung KY, Liu Y, Ren B, et al. Interferon regulatory factor-1-induced apoptosis mediated by a ligand-independent fas-associated death domain pathway in breast cancer cells. Oncogene. 2007; 26:6420–30. [PubMed: 17452973]
30. Nedjic J, Aichinger M, Emmerich J, Mizushima N, Klein L. Autophagy in thymic epithelium shapes the T-cell repertoire and is essential for tolerance. Nature. 2008; 455:396–400. [PubMed: 18701890]
31. Nedjic J, Aichinger M, Klein L. Autophagy and T cell education in the thymus: eat yourself to know yourself. Cell Cycle. 2008; 7:3625–8. [PubMed: 19029805]
32. Kraus WL, Kadonaga JT. p300 and estrogen receptor cooperatively activate transcription via differential enhancement of initiation and reinitiation. Genes & development. 1998; 12:331–42. [PubMed: 9450928]
33. Cameron DA, Keen JC, Dixon JM, Bellamy C, Hanby A, Anderson TJ, et al. Effective tamoxifen therapy of breast cancer involves both antiproliferative and pro-apoptotic changes. Eur J Cancer. 2000; 36:845–51. [PubMed: 10785588]
34. Ellis PA, Smith IE, Detre S, Burton SA, Salter J, A'Hern R, et al. Reduced apoptosis and proliferation and increased Bcl-2 in residual breast cancer following preoperative chemotherapy. Breast cancer research and treatment. 1998; 48:107–16. [PubMed: 9596482]
35. Pattingre S, Tassa A, Qu X, Garuti R, Liang XH, Mizushima N, et al. Bcl-2 antiapoptotic proteins inhibit Beclin 1-dependent autophagy. Cell. 2005; 122:927–39. [PubMed: 16179260]
36. Musgrove EA, Sutherland RL. Biological determinants of endocrine resistance in breast cancer. Nature reviews Cancer. 2009; 9:631–43.
37. Zhang L, Cardinal JS, Bahar R, Evankovich J, Huang H, Nace G, et al. Interferon regulatory factor-1 regulates the autophagic response in LPS-stimulated macrophages through nitric oxide. Mol Med. 2012; 18:201–8. [PubMed: 22105605]
38. Maiuri MC, Zalckvar E, Kimchi A, Kroemer G. Self-eating and self-killing: crosstalk between autophagy and apoptosis. Nature reviews Molecular cell biology. 2007; 8:741–52.
39. Bonapace L, Bornhauser BC, Schmitz M, Cario G, Ziegler U, Niggli FK, et al. Induction of autophagy-dependent necroptosis is required for childhood acute lymphoblastic leukemia cells to overcome glucocorticoid resistance. The Journal of clinical investigation. 2010; 120:1310–23. [PubMed: 20200450]
40. Papa L, Germain D. Estrogen receptor mediates a distinct mitochondrial unfolded protein response. Journal of cell science. 2011; 124:1396–402. [PubMed: 21486948]

Author Manuscript Author Manuscript Author Manuscript Author Manuscript

41. Teschendorff AE, Gomez S, Arenas A, El-Ashry D, Schmidt M, Gehrmann M, et al. Improved prognostic classification of breast cancer defined by antagonistic activation patterns of immune response pathway modules. BMC cancer. 2010; 10:604. [PubMed: 21050467]

42. Gao J, Wang Y, Xing Q, Yan J, Senthil M, Akmal Y, et al. Identification of a natural compound by cell-based screening that enhances interferon regulatory factor-1 activity and causes tumor suppression. Molecular cancer therapeutics. 2011; 10:1774–83. [PubMed: 21817116]

Author Manuscript Author Manuscript Author Manuscript Author Manuscript

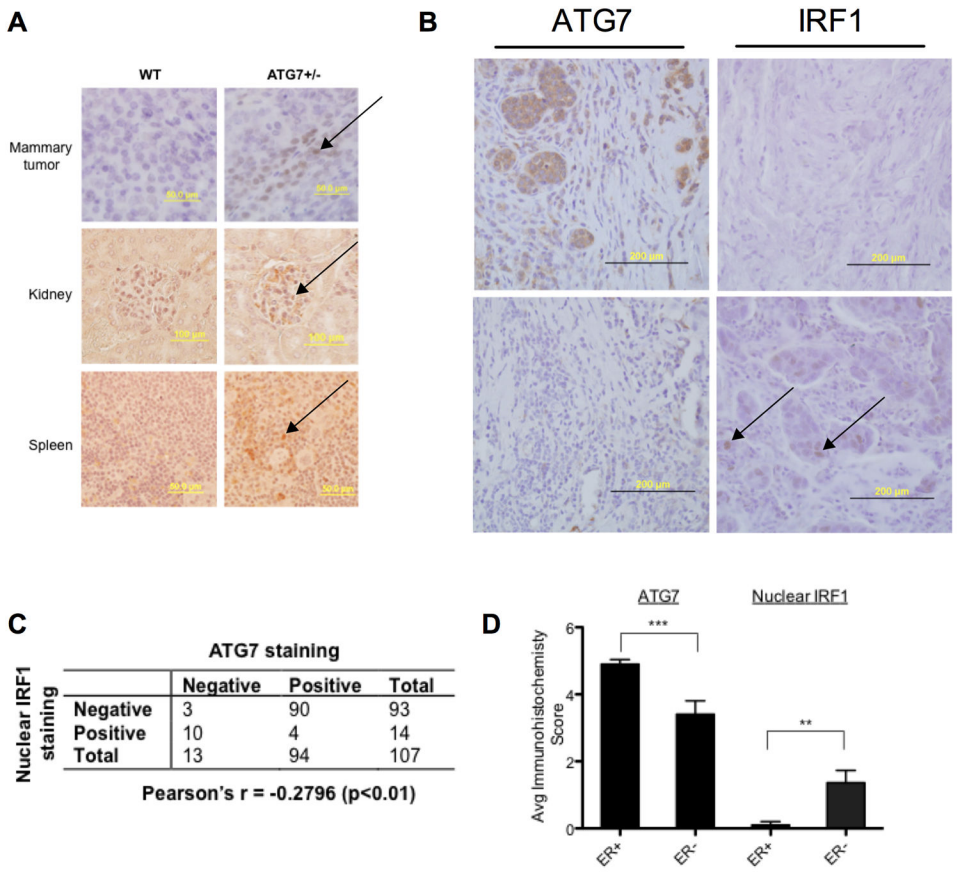

Fig. 1.

Nuclear IRF1 and ATG7 are inversely correlated *in vivo* and in human breast cancers. A, Immunohistochemical staining of IRF1 in wild-type (WT) and *ATG7* +/- mouse mammary tumors (top panel), kidney (middle panel), and spleen (bottom panel). Positive cells were quantified using ImageJ software. $n = 3$. B, Immunohistochemical staining of ATG7 (left) and IRF1 (right) in matched human breast cancer tissues. Arrows indicate nuclear IRF1 staining. C, Tissue sections of 107 breast cancer cores were immunostained for the expression of ATG7 and IRF1 and their correlation was analyzed by Pearson's rank correlation ($P < 0.01$). D, Average immunohistochemical score. $n = 52$; $^{**}P < 0.01$, $^{***}P < 0.001$ between indicated groups.

Author Manuscript Author Manuscript Author Manuscript Author Manuscript

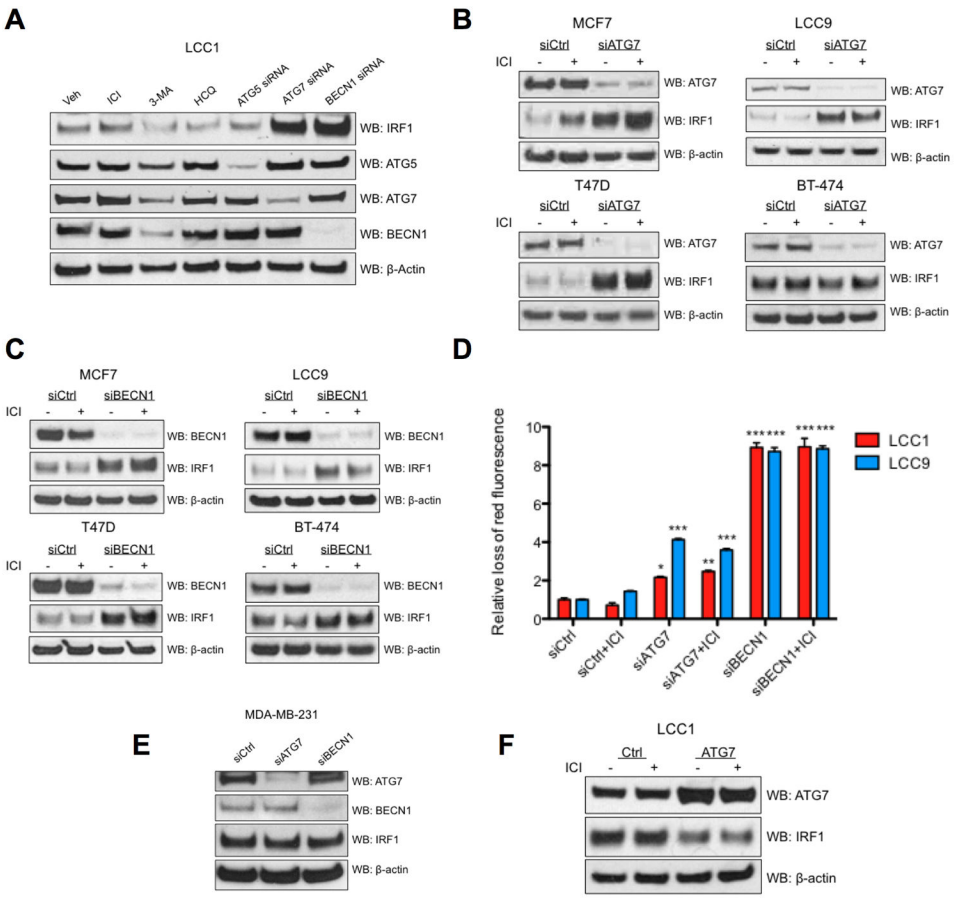

Fig. 2.

ATG7 and BECN1 inhibit IRF1 and apoptosis in human ER+ breast cancer cells. A, Western blot images of IRF1, ATG5, ATG7, and BECN1 in LCC1 cells treated with vehicle, 100 nM ICI, 5 mM 3-MA, 10 μM HCQ, or transfected with ATG5, ATG7, or BECN1 siRNA for 48 hours. B-C, MCF7, LCC9, T47D, and BT-474 were transfected with Ctrl, ATG7 siRNA (B) or BECN1 siRNA (C) and the following day, treated with 100 nM ICI for 48 hours. Western blot hybridization was used to measure IRF1, ATG7, and BECN1 protein expression. D, Mitochondrial permeability assay measured by flow cytometry in LCC1 and LCC9 cells transfected with ATG7, BECN1, or control (Ctrl) siRNA. E, IRF1 expression was measured in MDA-MB-231 cells transfected with ATG7, BECN1, or Ctrl siRNA. F, LCC1 cells transfected with ATG7 cDNA or empty vector were treated with 100 nM ICI for 48 hours and expression of IRF1 and ATG7 were analyzed by Western blot. β-actin served as the loading control. $n = 3$ independent experiments; $^{*}P < 0.05$, $^{**}P < 0.01$, $^{***}P < 0.001$ versus control/vehicle experiment.

Author Manuscript Author Manuscript Author Manuscript Author Manuscript

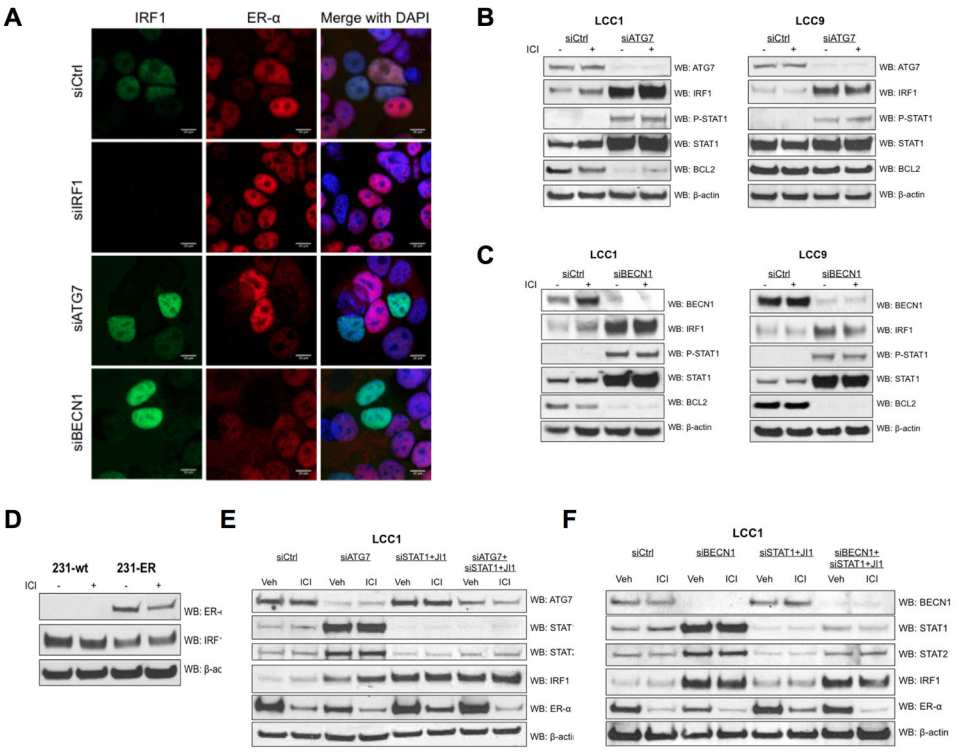

Fig. 3.

ATG7 and BECN1 knockdown causes IRF1 nuclear localization. A, LCC1 cells transfected with IRF1, ATG7, BECN1, or Ctrl siRNA were used to determine IRF1 and ERα localization by immunofluorescent confocal microscopy. B-C, LCC1 and LCC9 cells with transfected with Ctrl, ATG7 (B) or BECN1 siRNA (C) and treated with 100 nM ICI for 48 hours. Western blot hybridization of protein homogenates was used to measure IRF1, ATG7, BECN1, STAT1, P-STAT1, and BCL2. D, MDA-MB-231 cells were transfected with ERα or control cDNA and treated with vehicle or 100 nM ICI for 48 hours. Western blot hybridization of protein homogenates was used to measure ERα and IRF1 expression. E, Western blot images of LCC1 cells transfected with Ctrl, ATG7, STAT1, ATG7+STAT1 siRNA and treated with vehicle 100 nM ICI, or 15 nM JAK inhibitor (JI1) for 48 hours. β-actin served as the loading control. *n* = 3 independent experiments.

Author Manuscript Author Manuscript Author Manuscript Author Manuscript

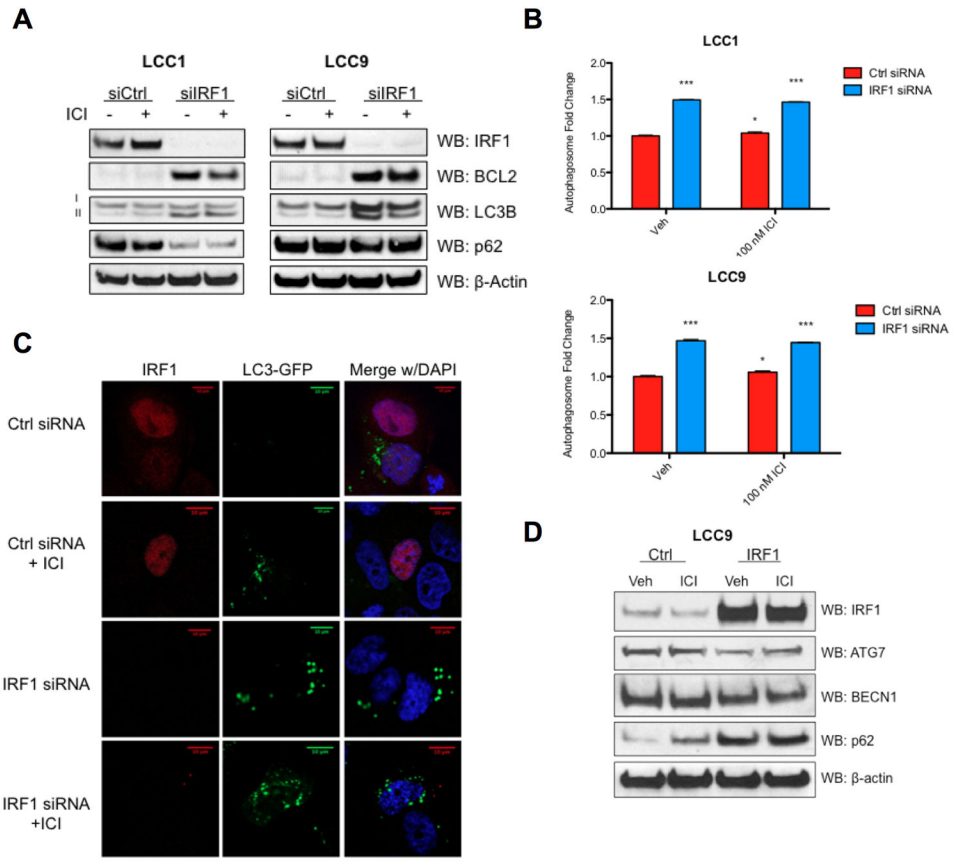

Fig. 4.

IRF1 knockdown induces autophagy. A, LCC1 and LCC9 cells were transfected with IRF1 siRNA and treated with 100 nM ICI for 48 hours. Western blot analysis of protein homogenates was used to measure expression of IRF1, BCL2, LC3B, and p62. B, Autophagosome formation assay in LCC1 and LCC9 cells transfected with IRF1 or Ctrl siRNA and treated with 100 nM ICI. Data are presented as percentage of total cells positive for green fluorescence; $n = 3$; $*P < 0.05$, $***P < 0.001$ versus control/vehicle experiment. C, LCC1 cells were transfected with IRF1/Ctrl siRNA and LC3-GFP and then treated with ICI. D, LCC9 cells were transfected with IRF1 or control cDNA and treated with 100 nM ICI. Representative Western blot images of indicated proteins. Equivalent protein loading was assessed by measuring β-actin. $n = 3$ independent experiments.

Author Manuscript Author Manuscript Author Manuscript Author Manuscript

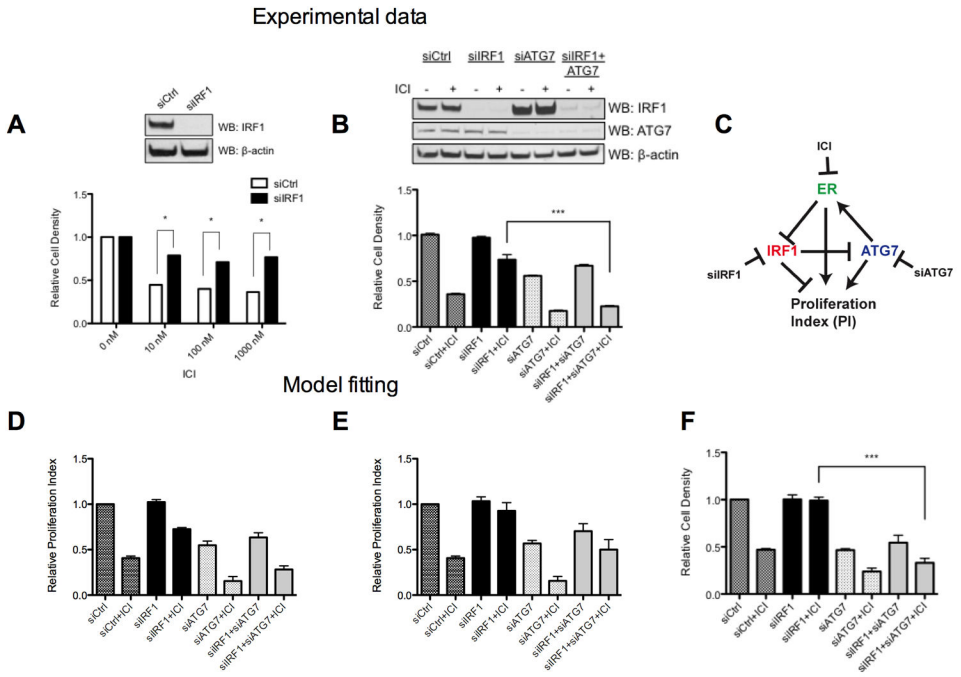

Fig. 5.

Mathematical modeling of proliferation data and experimental validation. A, LCC1 cells transfected with IRF1 or Ctrl siRNA were treated with vehicle control or ICI for 6 days and cell density measured by crystal violet. B, LCC1 cells transfected with Ctrl, IRF1, ATG7, or IRF1+ATG7 siRNA were treated with vehicle control or 100 nM ICI for 6 days before analysis by crystal violet assay. Relative cell densities of each case are plotted. Western blot analysis shows each knockdown target of interest. $n = 3$ independent experiments; $^{*}P < 0.05$, $^{***}P < 0.001$ versus indicated groups. C, Wiring diagram of model. D, Model predictions for increasing the concentration of siATG7 by a factor of 2. E, Predictions for increasing the concentration of siIRF1 by a factor of 3. F, Experimental results for increasing the concentration of siIRF1 by a factor of 3. $n = 3$ independent experiments; $^{***}P < 0.001$ versus indicated groups

Author Manuscript Author Manuscript Author Manuscript Author Manuscript

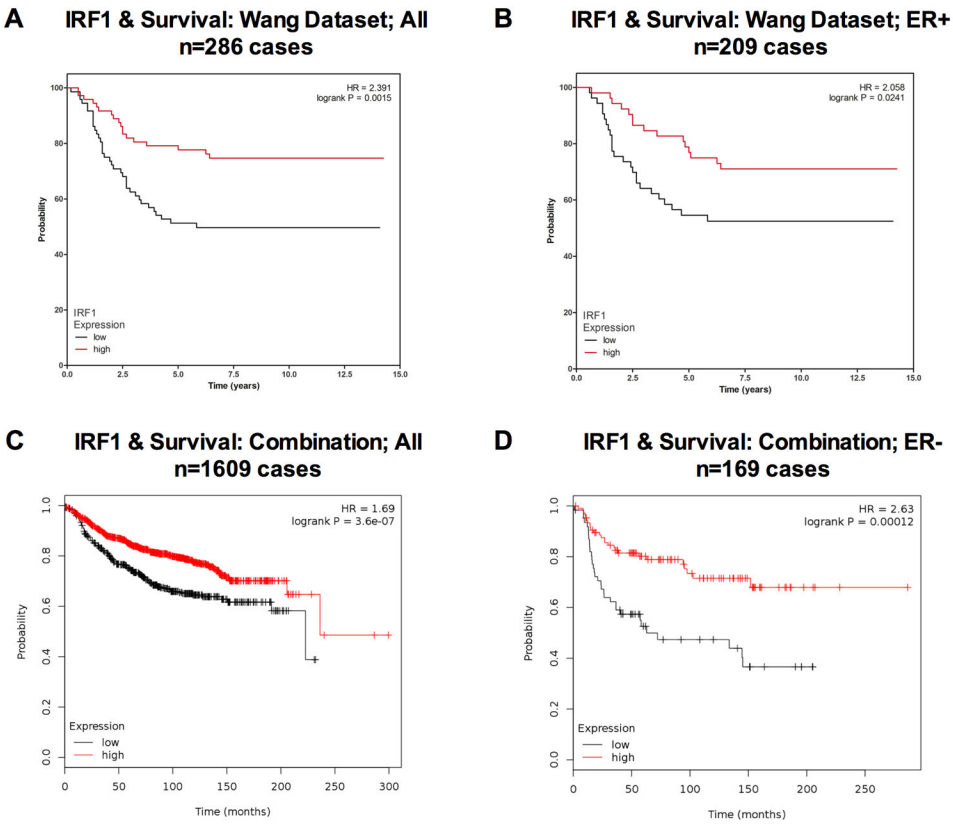

Fig. 6.

High IRF1 expression is associated with prolonged survival in human datasets. A-B, Kaplan-Meier plots show survival analysis for IRF1 expression using the Wang *et al.* dataset. 286 samples were split into quartiles according to IRF1 expression level (A). 209 samples with ER+ status were split and analyzed the same way (B). C-D, Several datasets were combined using the Kaplan-Meier Plotter and IRF1 expression was analyzed in the total population (C) and ER- subgroup (D).